



ARE YOU A
**SCIENTIFIC
REBEL?**



Unleash your true potential
with the new **CytoFLEX LX**
Flow Cytometer

DARE TO EXPLORE



**BECKMAN
COULTER**
Life Sciences



The Journal of
Immunology

Hyaluronan Binding Identifies a Functionally Distinct Alveolar Macrophage –like Population in Bone Marrow–Derived Dendritic Cell Cultures

This information is current as of July 25, 2017.

Grace F. T. Poon, Yifei Dong, Kelsey C. Marshall, Arif Arif, Christoph M. Deeg, Manisha Dosanjh and Pauline Johnson

J Immunol 2015; 195:632-642; Prepublished online 17 June 2015;

doi: 10.4049/jimmunol.1402506

<http://www.jimmunol.org/content/195/2/632>

References This article **cites 52 articles**, 27 of which you can access for free at:
<http://www.jimmunol.org/content/195/2/632.full#ref-list-1>

Subscription Information about subscribing to *The Journal of Immunology* is online at:
<http://jimmunol.org/subscription>

Permissions Submit copyright permission requests at:
<http://www.aai.org/About/Publications/JI/copyright.html>

Email Alerts Receive free email-alerts when new articles cite this article. Sign up at:
<http://jimmunol.org/alerts>

The Journal of Immunology is published twice each month by
The American Association of Immunologists, Inc.,
1451 Rockville Pike, Suite 650, Rockville, MD 20852
Copyright © 2015 by The American Association of
Immunologists, Inc. All rights reserved.
Print ISSN: 0022-1767 Online ISSN: 1550-6606.



Hyaluronan Binding Identifies a Functionally Distinct Alveolar Macrophage–like Population in Bone Marrow–Derived Dendritic Cell Cultures

Grace F. T. Poon,¹ Yifei Dong, Kelsey C. Marshall, Arif Arif, Christoph M. Deeg, Manisha Dosanjh, and Pauline Johnson

Although classical dendritic cells (DCs) arise from distinct progenitors in the bone marrow, the origin of inflammatory DCs and the distinction between monocyte-derived DCs and macrophages is less clear. In vitro culture of mouse bone marrow cells with GM-CSF is a well-established method to generate DCs, but GM-CSF has also been used to generate bone marrow–derived macrophages. In this article, we identify a distinct subpopulation of cells within the GM-CSF bone marrow–derived DC culture based on their ability to bind hyaluronan (HA), a major component of the extracellular matrix and ligand for CD44. HA identified a morphologically distinct subpopulation of cells within the immature DC population (CD11c⁺ MHC II^{mid/low}) that were CCR5⁺/CCR7⁻ and proliferated in response to GM-CSF, but, unlike immature DCs, did not develop into mature DCs expressing CCR7 and high levels of MHC II, even after stimulation with LPS. The majority of these cells produced TNF- α in response to LPS but were unable to activate naive T cells, whereas the majority of mature DCs produced IL-12 and activated naive T cells. This HA binding population shared many characteristics with alveolar macrophages and was retained in the alveolar space after lung instillation even after LPS stimulation, whereas the MHC II^{high} mature DCs were found in the draining lymph node. Thus, HA binding in combination with MHC II expression can be used to identify alveolar-like macrophages from GM-CSF–treated bone marrow cultures, which provides a useful in vitro model to study alveolar macrophages. *The Journal of Immunology*, 2015, 195: 632–642.

Macrophages and dendritic cells (DCs) are key regulators of the immune system (1, 2). Macrophages and immature DCs are key sentinel cells in the tissues where they help maintain tissue homeostasis. They sense damage and infection, and are highly phagocytic. In response to damage or microbial-associated molecules, macrophages initially promote an innate inflammatory response by producing proinflammatory cytokines such as TNF- α and IL-6 (3). Later on in the response, macrophages contribute to the healing and repair phase, in part by the production of anti-inflammatory cytokines IL-10 and TGF- β (4). DCs are specialized in the ability to process Ag and migrate to the peripheral lymphoid organs where they present Ag and activate naive T cells. Proinflammatory stimuli such as LPS result in IL-12 production by the DC, which polarizes T cells to make a Th1 response (5). Previously, the surface markers F4/80 and CD11b were used to broadly identify macrophages, and CD11c

and MHC II^{high} to identify DCs, but data now indicate this is an oversimplification as considerable phenotypic heterogeneity is apparent among macrophages and DCs in vivo (6–9). Specific environments and the cytokine milieu likely contribute to this phenotypic, and possibly functional, heterogeneity. For example, the addition of IL-4 to M-CSF–induced bone marrow–derived macrophages (BMDMs) upregulates CD11c and downregulates F4/80 (10). Whereas peritoneal and splenic red pulp macrophages are positive for F4/80 and CD11b, alveolar macrophages express low levels of these classical macrophage markers and high levels of CD11c (6, 11). Similarly, some DC subsets in the small intestine and lung have been reported to express F4/80 and CD11b (12, 13). Thus, based on these cell-surface markers alone, it is not possible to distinguish between DCs and macrophages, and there is still confusion in the field as to what is called a macrophage or DC (7–9). It has become clear that additional characterization including functional readouts is necessary to distinguish subsets of macrophages and DCs (6, 7). There has been considerable effort to map the gene expression profile of DCs and macrophages, and in this respect the ImmGen database (<http://www.immgen.org>) has become a useful resource to identify genes associated with a particular subset of cells. This microarray analysis of in vitro and ex vivo isolated populations has led to the identification of additional markers such as CD64 being used to identify macrophages (14, 15) and key transcription factors such as Zbtb46, together with Flt3R, c-Kit, and CCR7, to identify classical DCs (12). Despite these advances, a combination of phenotypic and functional characteristics is required to distinguish particular subsets of myeloid cells, and still these can be influenced by the microenvironment of the immune cell.

In vitro mouse models to generate BMDMs and bone marrow–derived DCs (BMDCs) are well established using M-CSF, GM-CSF, GM-CSF and IL-4, or Flt3 (16–19). Human blood monocytes can also give rise to macrophages by culturing with M-CSF or

Department of Microbiology and Immunology, University of British Columbia, Vancouver, British Columbia, Canada V6T 1Z3

¹Current address: Terry Fox Laboratory, British Columbia Cancer Agency, Vancouver, BC, Canada.

Received for publication October 1, 2014. Accepted for publication May 13, 2015.

This work was supported by the Canadian Institutes of Health Research (Grant MOP-119503) and summer studentships from the Natural Sciences and Engineering Council of Canada (to Y.D., K.C.M., and A.A.).

Address correspondence and reprint requests to Dr. Pauline Johnson, Department of Microbiology and Immunology, University of British Columbia, 2350 Health Sciences Mall, Life Sciences Centre, Vancouver, BC, Canada V6T 1Z3. E-mail address: pauline@mail.ubc.ca

Abbreviations used in this article: BAL, bronchoalveolar lavage; BMDC, bone marrow–derived DC; BMDM, bone marrow–derived macrophage; DC, dendritic cell; FI-HA, fluorescein-conjugated hyaluronan; HA, hyaluronan; UBC, University of British Columbia.

Copyright © 2015 by The American Association of Immunologists, Inc. 0022-1767/15/\$25.00

GM-CSF (20), and to DCs by culturing in GM-CSF and IL-4 (21). Murine GM-CSF bone marrow cultures lead to the generation of CD11b⁺ CD11c⁺ DCs, but lack the CD8⁺ and CD4⁺ subpopulations of classical DCs, as well as the plasmacytoid DCs that are found in lymphoid tissue. These cells are better represented in the Flt3-induced BMDC culture (22). Thus, the GM-CSF-induced BMDCs are perhaps more representative of the *in vivo* monocyte-derived DCs that produce TNF- α and NO and are referred to as inflammatory DCs (23, 24). M-CSF- and GM-CSF-generated macrophages produce distinct cytokines in response to LPS, suggesting that GM-CSF-generated macrophages are more proinflammatory and the M-CSF macrophages more anti-inflammatory (16, 20). Thus, it is not clear what these *in vitro* cultures best represent *in vivo*.

Activated human blood monocytes and M1 (LPS and IFN- γ) and M2 (IL-4) polarized M-CSF-induced murine BMDMs have been shown to bind hyaluronan (HA), a major component of the extracellular matrix (10, 25). HA is present in virtually all tissues. It is a glycosaminoglycan consisting of repeating units of β (1, 4)-D-glucuronic acid and β (1, 3)-N-acetyl-D-glucosamine, and in homeostasis is present in tissues in its high molecular mass form (>1000 kDa) where it is very hygroscopic and plays a key role in tissue hydration (26). Upon tissue injury or infection, HA becomes fragmented and HA synthesis increases (27), and the persistence of HA fragments is associated with unresolved inflammation (28) as high molecular mass HA is normally restored on wound healing and tissue repair. CD44 is the major cell-surface receptor for HA on immune cells, but not all CD44-expressing cells bind HA (29, 30). On human monocytes, CD44 can be induced to bind HA by various inflammatory cytokines including GM-CSF, IL-1 α and IL-1 β , and TNF- α (25, 31), and M-CSF-derived BMDMs only bind HA after they are stimulated with M1 or M2 polarizing agents (10). However, the functional significance of this induced binding remains enigmatic. Although DCs respond to fragmented HA (4-14 oligosaccharides) in a TLR-4-dependent manner (32, 33), it is not known whether CD44 on immature and mature DCs interacts with HA or whether HA helps mediate DC-T cell interactions, as Pep-1, a positively charged peptide that blocks HA binding to CD44, inhibited T cell proliferation (34). Given that HA binds to activated monocytes and polarized M-CSF macrophages, and has been linked with DC maturation and T cell activation, we sought to further analyze the HA binding abilities of GM-CSF-induced BMDCs using fluorescently labeled HA and flow cytometry. We found that only a subpopulation of CD11c⁺ MHC II^{mid/low} cells bound HA. Further investigation revealed these cells to be functionally distinct from DCs and instead more closely aligned functionally and phenotypically with alveolar macrophages. This work provides a new marker to identify GM-CSF-induced macrophages from immature DCs and illustrates the heterogeneity present within GM-CSF-derived bone marrow DC cultures. It also provides a means to identify and isolate these cells that can be used as an *in vitro* model for alveolar macrophages, which are difficult to obtain in significant numbers from the lung or bronchoalveolar lavage (BAL).

Materials and Methods

Mice

C57BL/6J mice and C57BL/6-transgenic (TeraTerb) 425Cbn/J mice with a TCR specific for chicken OVA peptide₃₂₃₋₃₃₉ (referred to as OT-II mice) were purchased from the Jackson Laboratories, C57BL/6-transgenic mice ubiquitously expressing GFP from a β -actin CMV hybrid promoter (referred to as GFP⁺ mice) were a kind gift from F. Rossi, and all were bred in-house. CD44-deficient (CD44^{-/-}) mice (35) were backcrossed onto the C57BL/6J background for nine generations. Animals were initially housed in the Wesbrook Animal Unit and later transferred to the Centre for Disease Modeling at the University of British Columbia (UBC). Mice used for experiments were between 6 and 15 wk of age. All animal experiments

were conducted in accordance with the Canadian Council of Animal Care Guidelines using protocols approved by the University Animal Care Committee.

Reagents

Recombinant mouse CCL3 and CCL19 were from R&D Systems. *Escherichia coli* 0111:B4 LPS was from Invivogen or Sigma-Aldrich (catalog no. L4391). Tissue culture supernatant from J558L cells was the source of GM-CSF (36). Brefeldin A from *Penicillium brefeldianum* was from Sigma-Aldrich. Dextran labeled with Alexa Fluor 647 was from Invitrogen. Fluorescein-conjugated HA (Fl-HA) was prepared as described previously (37) using rooster comb hyaluronic acid sodium salt from Sigma-Aldrich (H5388). Specific high molecular mass HA (1.68×10^6 Da) was from Lifecore Biomedical and conjugated with Alexa Fluor 647 by the Antibody Laboratory at UBC.

Abs

The following Abs against mouse Ags were used for flow cytometry or cell isolation: B220 (RA-6B2), Ter 119 (Ter119), CD8 α (53.67), F4/80 (BM8), CD115 (Af598), CD11b (M1/70), CD11c (N418), Gr1 (RB6-8C5), CD86 (P03.1), MHC II (M5/114.15.2), CD44 (IM7), Ly6C (AL21), Ly6G (1A8), CD200R (OX110), CD206 (C068C2), Siglec-F (E50-2440), CCR5 (7A4), CCR7 (4B12), TNF- α (MP6-XT22), IL-6 (MP5-20F3), and IL-12 (p40, C17.8). Abs with the exception of IM7 and the Fc receptor blocking Ab, 2.4G2 tissue culture supernatant, were purchased from eBioscience, BioLegend, BD Pharmingen, or Antibody Laboratory at UBC. Abs were conjugated to FITC, PE, PerCP-eFluor 710 (PerCP), PE/cyanine 7 (PE/Cy7), allophycocyanin, Pacific blue, or biotin. Biotin-conjugated Abs were detected with fluorescently labeled streptavidin from eBioscience. Purified CD44 mAb was conjugated to Pacific blue fluorescent dye according to the manufacturer's instructions (Molecular Probes).

Cell isolation

Mice were euthanized by isoflurane overdose and alveolar cells were harvested from the BAL by catheterization of the trachea and washing three times, each with 1 ml PBS, 1% BSA, and 2 mM EDTA. Between 80 and 95% of the cells in the BAL were alveolar macrophages. Cells were pelleted, then treated with RBC lysis buffer (0.84% ammonium chloride, 2 mM Tris-Cl pH 7.2) for 5 min at room temperature.

Transgenic CD4 T cells were isolated from the spleen of OT-II mice. In brief, the spleen was minced and pressed through a strainer, and then treated with RBC lysis buffer. Cells were resuspended in PBS with 0.5% BSA and 2 mM EDTA, incubated with 2.4G2 for 20 min, then labeled with biotinylated Abs against B220, CD8 α , CD11b, CD11c, and Ter119, followed with anti-biotin magnetic beads (Miltenyi Biotec). The negative fraction was collected from MACS LS columns according to manufacturer's instructions (Miltenyi Biotec). Typically, the OT-II CD4 T cells had $\geq 85\%$ purity.

Generation of GM-CSF-derived BMDCs

BMDCs were prepared according to Lutz et al. (18), with slight modifications. Bone marrow cells were isolated from the femurs and tibias of mice, treated with RBC lysis buffer, and then cultured in RPMI 1640 (Invitrogen), containing 10% heat-inactivated serum FCS (Invitrogen), 20 mM Hepes (Invitrogen), 1 \times nonessential amino acid (Invitrogen), 55 μ M 2-ME (Invitrogen), 50 U/ml penicillin/streptomycin (Invitrogen), 1 mM sodium pyruvate, 2 mM L-glutamine, and 2-4% GM-CSF containing supernatant, from J558L cells transfected with the GM-CSF gene (hereafter referred to as GM-CSF). The induction of HA binding in BMDC culture was also confirmed using 20 ng/ml rGM-CSF (Cedarlane). A total of 2×10^5 cells/ml was cultured in 10 ml in a 100 \times 15-mm petri dish (Falcon), or in 40 ml in a 150 \times 15-mm petri dish (Falcon). Half of the media was changed on days 3 and 6 (and day 9 when necessary) by spinning down the cells and resuspending in fresh media with GM-CSF. Nonadherent cells were harvested at the indicated time points. A typical yield on day 7 would be 5×10^6 and 25×10^6 cells for 10- and 40-ml cultures, respectively, with $\sim 70\%$ CD11c⁺ cells.

Flow cytometry

Cells from BMDC cultures ($2-10 \times 10^5$) were kept at 4°C and incubated with 2.4G2 Fc receptor blocking Ab for 20 min, washed with FACS buffer (1 \times PBS, 2 mM EDTA and 2% BSA), and then labeled with mAbs at predetermined dilutions for 20 min protected from light. This step was repeated if labeling with secondary Ab was required. After washing, cells were resuspended in FACS buffer containing 0.1-0.2 μ g/ml propidium iodide (Sigma-Aldrich) or DAPI (Sigma-Aldrich) to label nonviable cells.

Cells were analyzed on the LSR II (BD Biosciences) or MACSQuant (Miltenyi Biotec) flow cytometers and analyzed using FlowJo (Tree Star) software. Negative controls for flow cytometry were unstained cells or CD44^{-/-} cells for HA binding, isotype or unstimulated cells for intracellular cytokine production, and unstained or fluorescence minus one controls for cell-surface markers.

Measurement of dextran uptake by flow cytometry

Cells from day 9 BMDC cultures (2×10^5) were plated in 200 μ l DC media without GM-CSF and incubated with 10 μ g/ml Alexa Fluor 647-conjugated dextran (Invitrogen) for 45 min at 37°C with 5% CO₂. Then cells were labeled with FI-HA (5 μ g/ml) and mAbs on ice to determine the HA binding ability and phenotype of cells that took up dextran.

Stimulation and measurement of intracellular cytokines in BMDCs

Nonadherent, day 7 BMDCs (2×10^5) and ex vivo cells collected from the BAL, which primarily consist of alveolar macrophages, were plated in 96-well nontissue culture-treated round-bottom plates in BMDC media (no GM-CSF) with or without 100 ng/ml LPS (Invivogen). BMDCs were stimulated for 8 h with LPS, and brefeldin A (10 μ g/ml) was added 2 h after LPS stimulation; then intracellular TNF- α , IL-6, and IL-12 production was measured by flow cytometry. Detection of intracellular TNF- α , IL-6, and IL-12 was performed after 4 h of LPS and brefeldin A treatment of ex vivo alveolar macrophages from BAL. Cells were harvested for flow cytometry after LPS stimulation by incubation with 2 \times Versene for 5 min at 37°C. Fc receptors were blocked with 2.4G2 for 20 min at 4°C; then the cells were surface labeled with a predetermined concentration of mAbs for 20 min. Cells were fixed in 4% paraformaldehyde (Canemco & Marivac) for 10 min, then permeabilized in 0.1% saponin for 10 min at room temperature before adding cytokine-specific mAbs in saponin buffer for 30 min at room temperature. Expression was measured after washing by flow cytometry (LSR II) and analyzed using FlowJo (Tree Star) software.

Cell imaging

Cells were cultured in 96-well tissue culture plates for 2 h at 37°C before images were acquired by a Leica microsystem AF 6000 microscope, using an N PLAN L 20 \times /0.35 dry objective lens.

In vitro Ag-specific T cell proliferation assay

Nonadherent cells from day 7 BMDC cultures were collected and sorted for different BMDC (CD11c⁺ Gr1⁻) populations based on their MHC II expression and HA binding ability. BMDCs or cells obtained from the BAL (5×10^3) were stimulated with 100 ng/ml LPS or not, in the presence or absence of 1 μ g/ml OVA₃₂₃₋₃₃₉ peptide overnight. The next day, supernatants from the BMDC culture were removed, and 5×10^4 CD4 OT-II T cells (isolated from spleen as described earlier and labeled with 10 μ M CFSE proliferation dye according to the manufacturer's instructions [Invitrogen]) were added. CD4 OT-II T cells and CD11c⁺ cells were cocultured at a 10:1 ratio for 3 d. The CFSE profile and the number of CD4⁺ T cells were analyzed by flow cytometry using the MACSQuant (Miltenyi Biotec).

Transwell migration assay

The transwell migration assays were performed using 24-well plates and inserts with 5- μ m pores (Costar). A total of 500 μ l media with or without the chemoattractants CCL3 (40 ng/ml; R&D systems) or CCL19 (40 ng/ml; R&D systems) was placed in the bottom of the well. A total of 5×10^5 nonadherent cells collected from day 8 BMDC cultures was resuspended in 100 μ l fresh BMDC media and placed onto the insert. Then cells were incubated at 37°C for 2 h in CCL19 experiments, and 3 or 24 h in CCL3 experiments. Cells that migrated out of the inserts were collected and analyzed for their phenotype and counted using the MACSQuant (Miltenyi Biotec). To determine the total number of cells recovered, we placed 5×10^5 cells in 500 μ l media into the bottom of the well, then collected and counted them: % migration = number of cells migrated in the presence or absence of chemokine/total number of cells recovered \times 100.

BMDC in vitro cultures

To characterize the phenotypes and proliferation of the BMDC subsets, we harvested nonadherent cells from day 7 BMDC cultures and labeled them with FI-HA, CD11c, Gr1, MHC II mAb, and propidium iodide (Sigma-Aldrich) as described earlier. Different BMDC (CD11c⁺ Gr1⁻) populations were sorted by FACS, and equal numbers of cells ($\sim 5 \times 10^4$) from each subset were plated in 96-well plates in the presence of GM-CSF, in 200 μ l BMDC media. GM-CSF was added to the cultures 3 d after cell

sorting (day 10 BMDCs). Cells were analyzed by flow cytometry at specific time points. The number and phenotype of cells were acquired by MACSQuant (Miltenyi Biotec) and then analyzed using FlowJo (Tree Star, Ashland, OR) software.

Different BMDC (CD11c⁺ Gr1⁻) populations were sorted by FACS, labeled with or without 10 μ M CFSE proliferation dye according to the manufacturer's instructions (Invitrogen), to study the effect of LPS on specific MHC II/HA binding subsets. Equal numbers of cells ($\sim 5 \times 10^4$) from each subset were plated in 96-well plates in the presence or absence of 100 ng/ml LPS (Invivogen) in 200 μ l BMDC media and analyzed by flow cytometry at the specified time points.

Instillation of GM-CSF BMDCs into the lung

The nonadherent cells from day 8 GM-CSF BMDC cultures derived from GFP⁺ bone marrow cells were collected, resuspended in sterile PBS, and 5×10^6 cells/50 μ l PBS were instilled into the lungs of C57BL/6J mice. Twenty-four hours later, some animals were further challenged with 25 μ g LPS in 50 μ l PBS via intratracheal instillation (38). The BAL and mediastinal lymph node were collected 24 h after LPS challenge and analyzed by flow cytometry.

Statistics

Data shown are the average \pm SD. Significance was determined by a Student two-tailed, unpaired *t* test with **p* < 0.05, ***p* < 0.01, ****p* < 0.001, unless otherwise specified.

Results

GM-CSF induces HA binding in BMDC cultures

Flow cytometry of ex vivo bone marrow cells with FI-HA revealed a small percentage of HA binding cells that increased upon culture with GM-CSF (Fig. 1A). On day 4, $\sim 85\%$ of the HA binding cells were CD115⁺ Ly6C⁺ Ly6G⁻, indicative of a monocyte population (Fig. 1B). However, at this stage, only 15% of the total monocyte population (CD115⁺ Ly6C⁺) bound HA. Early in a GM-CSF BMDC culture (days 0–5), the majority of the nonadherent cells were positive for Gr1, a marker of neutrophils and monocytes (data not shown). Over time, the proportion of Gr1⁺ cells in the culture decreased as the percentage of CD11c⁺ cells increased. The percentage of CD11c⁺ cells increased together with the percentage of HA binding cells (Fig. 1A). However, the HA binding population remained relatively constant from day 6, whereas the CD11c⁺ population continued to increase over time, indicating that not all CD11c⁺ cells bound HA.

In the GM-CSF BMDC cultures, both immature and mature DCs were present in the nonadherent fraction of the culture at day 7, identified by MHC II^{mid} expression for immature DCs, and MHC II^{high} together with the upregulation of costimulatory molecules such as CD40, CD80, and CD86 for mature DCs (18). In day 7 GM-CSF BMDC cultures, $\sim 70\%$ of the cells were CD11c⁺ Gr1⁻ (Fig. 1C). Examination of the FI-HA binding cells on day 7 revealed that only a subpopulation of the CD11c⁺ cells, primarily a portion of the MHC II^{mid/low} populations, bound HA (Fig. 1D). Furthermore, HA binding was dependent on the presence of the HA receptor, CD44, because BMDCs derived from CD44-deficient bone marrow cells did not bind HA (Fig. 1D). Although there was not a dramatic difference in CD44 expression between the high and low HA binding cells, when the histograms were overlaid, the HA binding cells did express slightly higher levels of CD44 (Fig. 1E). This indicates that CD44-dependent HA binding is induced on monocytes maturing in the presence of GM-CSF, and high FI-HA binding is apparent on a subpopulation of CD11c⁺ MHC II^{mid/low} cells.

HA binding MHC II^{mid/low} cells have characteristics of immature DCs

Further analysis of the CD11c population revealed that the majority of MHC II^{mid/low} cells were positive for the common monocyte and macrophage markers, CD115 and F4/80, whereas the mature

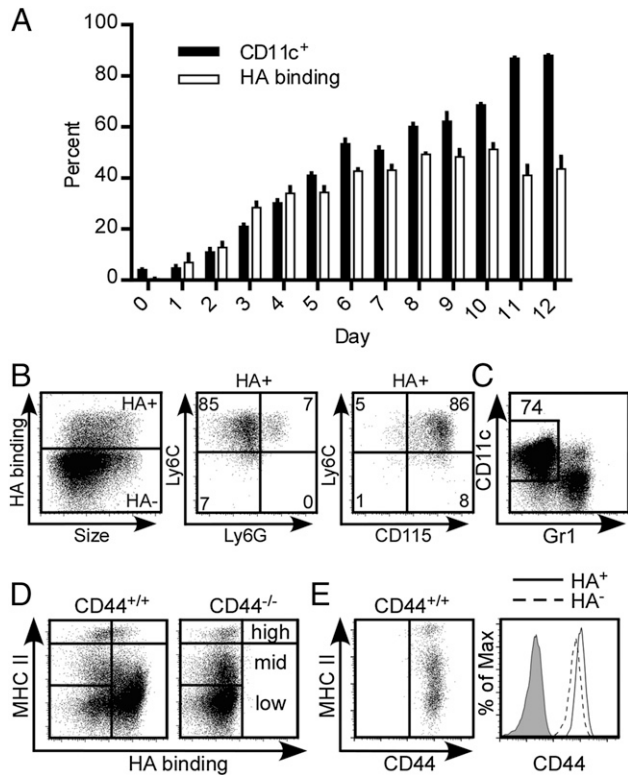


FIGURE 1. GM-CSF induces HA binding in BMDCs and HA binding identifies a subpopulation of CD11c⁺, MHC II^{mid/low} cells. C57BL/6J (CD44^{+/+}) and CD44^{-/-} bone marrow cells were cultured in the presence of GM-CSF for 12 d, and the phenotype and HA binding ability were analyzed daily by flow cytometry. **(A)** Percentage of CD11c⁺ and FI-HA binding cells over time. Graphs show the average ± SD of three mice from one experiment. **(B)** On day 4, Ly6C, Ly6G, and CD115 expression were analyzed on HA binding (HA⁺) cells. **(C)** Proportion of CD11c⁺ Gr1⁻ cells in a day 7 BMDC culture. **(D)** Day 7 CD11c⁺ Gr1⁻ cells were gated and the expression of MHC II and HA binding analyzed on CD44^{+/+} and CD44^{-/-} BMDCs. **(E)** MHC II and CD44 expression were analyzed on CD44^{+/+} BMDCs, and a histogram shows CD44 expression on HA binding and nonbinding cells. The shaded peak is a negative control using CD44^{-/-} cells. (A and E) Representative data from two experiments. (B–D) Data from one representative experiment, repeated at least three times.

MHC II^{high} CD11c^{high} population was negative for these markers and positive for the costimulatory marker, CD86 (Fig. 2A). To better characterize the HA binding population, we analyzed the expression of the chemokine receptor CCR5, known to be expressed on immature DCs, and CCR7 induced on mature DCs (39) by flow cytometry (Fig. 2B). As expected, the MHC II^{high} population was negative for CCR5 and positive for CCR7, whereas the MHC II^{mid/low} CD11c⁺ cells were largely negative for CCR7 and largely positive for CCR5, consistent with an immature DC phenotype. In transwell migration assays, the MHC II^{mid/low} immature DCs migrated toward the CCR5 ligand, CCL3, whereas MHC II^{high} mature DCs migrated toward the CCR7 ligand, CCL19 (Fig. 2C). Notably, within the MHC II^{mid/low} CCR5⁺ cells that migrated, a greater percentage of low HA binding cells migrated after 3 and 24 h compared with the high HA binding MHC II^{mid/low} DCs (Fig. 2D), indicating that the HA binding cells were less migratory to CCL3. This was our first indication that the MHC II^{mid/low} population may be heterogenous and HA binding may identify a functionally distinct population within the CD11c, MHC II^{mid/low} population.

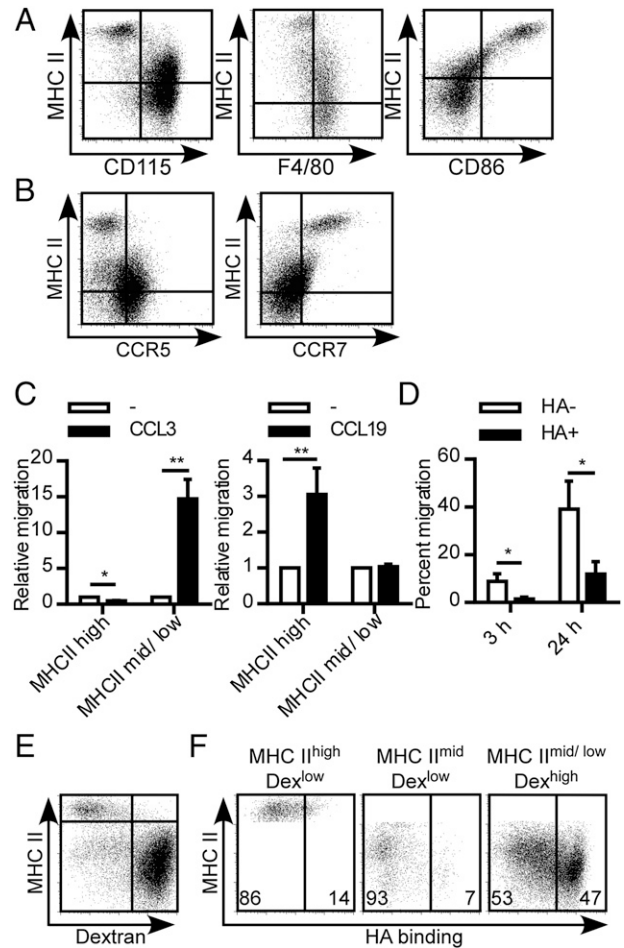


FIGURE 2. HA binding MHC II^{mid/low} cells have an immature DC phenotype but with less migratory ability. C57BL/6J bone marrow cells were cultured in the presence of GM-CSF for 7 or 9 d. **(A)** The expression of MHC II versus CD115, F4/80, and CD86 was analyzed on day 8 CD11c⁺ cells by flow cytometry. **(B)** Expression of MHC II versus CCR5 and CCR7 was analyzed on CD11c⁺ Gr1⁻ cells from day 7 cultures. **(C)** The migration of day 8 cells toward CCL19 after 2 h and CCL3 after 3 h was examined in transwell assays. Number of CD11c⁺ Gr1⁻ MHC II^{high} and MHC II^{mid/low} cells that migrated in the absence of chemokine was set to 1 to measure chemokine-specific migration. **(D)** Percentage of CD11c⁺ Gr1⁻ MHC II^{mid/low} HA binding (HA⁺) and MHC II^{mid/low} low HA binding (HA⁻) cells that migrated toward CCL3 after 3 and 24 h. **(E)** Day 9 cells were incubated with Alexa Fluor 649-conjugated dextran at 37°C for 45 min; the expression of MHC II and amount of dextran uptake were analyzed on CD11c⁺ cells. **(F)** HA binding ability of mature and immature DCs gated by MHC II expression and dextran in (E). Graphs show an average of three mice from one experiment ± SD with significance indicated as **p* < 0.05, ***p* < 0.01, using paired Student *t* test. Data shown are from one representative experiment, repeated at least three times.

Moreover, within the MHC II^{mid/low} population, some of the MHC II^{mid} cells expressed an intermediate maturation phenotype. These cells were largely low HA binding cells that were MHC II^{mid}, and by multiparameter labeling expressed low levels of CCR5 and F4/80 similar to a mature DC, but also expressed low levels of CCR7 and were not positive for CD86 (data not shown). This suggests that this population is an intermediate population between the mature and immature DCs, with the HA binding CD11c⁺ cells showing a more immature DC phenotype (Figs. 1D, 2A, 2B).

To further characterize the immature CD11c population, we examined the ability of DCs to undergo macropinocytosis and take

up dextran. Immature DCs take up more dextran than mature DCs (40). After a 45-min incubation with fluorescent dextran at 37°C, three major populations were separated by their MHC II expression and relative amount of dextran uptake (Dex): 1) MHC II^{high} Dex^{low}, 2) MHC II^{mid} Dex^{low}, and 3) MHC II^{mid/low} Dex^{high} (Fig. 2E). The majority of HA binding cells were present in the dextran high population, consistent with it labeling an immature DC population. Both dextran low populations were also low HA binding (Fig. 2F). Taken together, HA binding identifies an immature MHC II^{mid/low} CD11c⁺ DC population that does not express DC maturation markers (Figs. 1D, 2A, 2B), takes up dextran (Fig. 2F), and although it expresses CCR5, was less migratory toward CCL3 (Fig. 2D). Furthermore, high levels of MHC II correlated with lower HA binding ability.

HA binding cells do not develop into mature MHC II^{high} DCs

To test the hypothesis that DCs downregulate their ability to bind HA as they mature, we sorted day 7 CD11c⁺ Gr1⁻ cells into four populations based on their MHC II expression and HA binding ability, and then analyzed changes in HA binding over time. MHC II^{low} HA binding^{low} (p0), MHC II^{mid/low} HA binding^{high} (p1), MHC II^{mid} HA binding^{low} (p2), and MHC II^{high} HA binding^{low} (p3) BMDCs were sorted by FACS (Fig. 3A) and their CD44 expression levels were compared. As determined in Fig. 1E, the highest HA binding p1 population (shaded histogram) expressed the most CD44 on its surface, whereas the low HA binding populations expressed slightly lower levels of CD44 (Fig. 3B). To characterize the maturation of these cells, we monitored their MHC II expression and HA binding over time (Fig. 3C). Three days after sorting (day 10), the percentage of HA binding cells (p1) had decreased. However, this population never matured into MHC II^{high} DCs, even after 5 d (day 12). This was in contrast with the MHC II^{mid} HA binding^{low} population (p2) where the majority of cells rapidly became MHC II^{high} after 24 h, consistent with the expected maturation of immature DCs from MHC II^{mid} to MHC II^{high}. The MHC II^{low} HA binding^{low} population, p0, was also capable of giving rise to all the subsets including a small percentage of MHC II^{high} mature DCs (6% by day 12), consistent with it containing progenitors and immature DCs that are capable of responding to GM-CSF and generating mature DCs over the time studied. The majority of the MHC II^{high} HA binding^{low} (p3) cells remained MHC II^{high} and were short lived, as expected for mature DCs. Because the purity after cell sorting was 95–98%, it was possible that the MHC II^{high} population had a small percentage contamination from the p1 population, which became more prominent over time as the MHC II^{high} population declined in number.

Overall, this demonstrated that the low HA binding populations, p0 (MHC II^{low}) and p2 (MHC II^{mid}), were capable of maturing into the mature MHC II^{high} DCs, whereas the high HA binding MHC II^{low/mid} population was not.

Because LPS is a microbial-associated molecular pattern known to induce DC maturation, we sought to determine whether LPS would cause the p1 population to mature into MHC II^{high} DCs. Sorted day 7 cells were stimulated with 100 ng/ml LPS for 24 h and then analyzed by flow cytometry. LPS stimulated 22% of p0 cells and 45% of p2 cells to mature into MHC II^{high} cells compared with the untreated samples (Fig. 3D). In contrast, there was only a 6% increase in percentage of MHC II^{high} cells from the HA binding p1 population (Fig. 3D). Even though LPS upregulated MHC II expression in p1, it was not to the same extent as in the p2 and p3 populations, and although these cells upregulated the costimulatory molecules, CD40 and CD86, they did not express CCR7 (data not shown), indicating they were distinct from the mature DC population. In addition, the proportion of MHC II^{high}

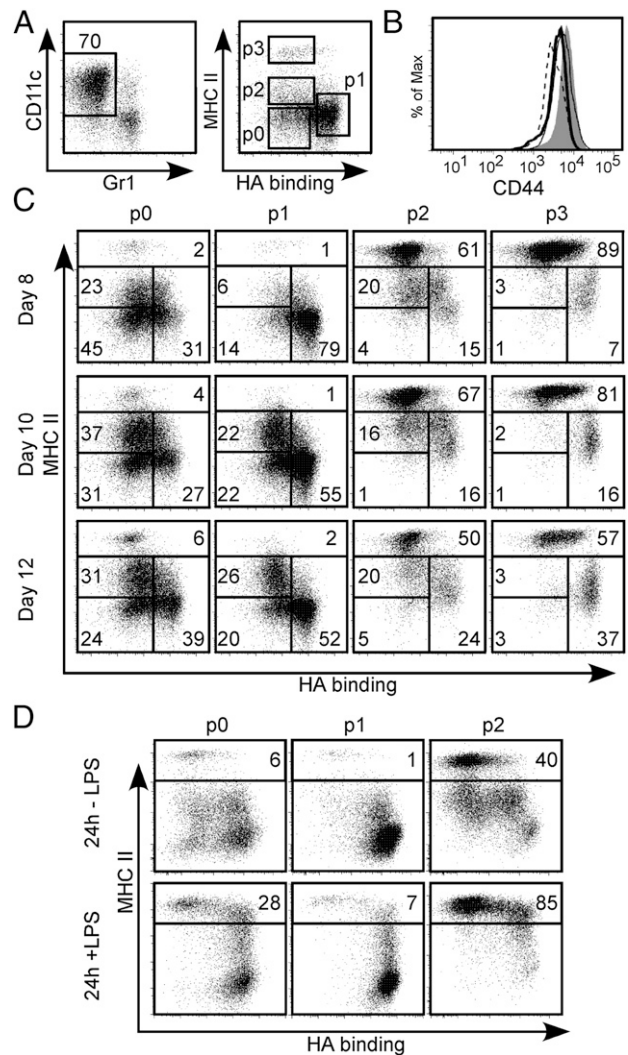


FIGURE 3. HA binding cells do not mature into MHC II^{high} DCs. Day 7 C57BL/6J BMDCs were sorted for CD11c⁺ Gr1⁻ MHC II^{low} HA binding^{low} (p0), MHC II^{mid/low} HA binding^{high} (p1), MHC II^{mid} HA binding^{low} (p2), and MHC II^{high} HA binding^{low} (p3) populations, as gated in (A). (B) CD11c⁺ day 8 BMDCs were gated, and the histogram shows the CD44 expression levels in p0 (solid thick line), p1 (shaded), p2 (dashed line), and p3 (solid line) by flow cytometry. (C) Approximately 5×10^4 cells from each population (as sorted in A) were plated and further cultured with fresh GM-CSF. MHC II expression and HA binding were analyzed 1 d (day 8), 3 d (day 10), and 5 d (day 12) later by flow cytometry. (D) A total of 5×10^4 cells from p0, p1, and p2 were plated and further cultured with fresh GM-CSF, with or without LPS (100 ng/ml) for 24 h. The expression of MHC II and HA binding were analyzed by flow cytometry. This is a representative plot that was repeated three times.

cells differentiated from p0 was greater than p1, suggesting p1 is not an intermediate population between the p0 and p3. Even after 3 d of stimulation, the HA binding cells did not express CCR7 or mature into MHC II^{high} DCs (data not shown). Together this shows that the low HA binding, MHC II^{low} and MHC II^{mid} cells can generate mature MHC II^{high} low HA binding DCs, whereas the high HA binding MHC II^{mid/low} population does not. This makes the HA binding, p1 population distinct from the typical immature DC population.

HA binding identifies a proliferative CD11c⁺ population

Sorted day 7 cells (p1–p3) were cultured in GM-CSF, and cell numbers were counted at days 8, 10, and 12. The numbers were

normalized to day 8 numbers and the p1 population showed a significant increase by day 10, whereas the p2 population did not, and the p3 population decreased (Fig. 4A). This indicates that the HA binding p1 population can proliferate in response to GM-CSF and p2 cells were either not proliferating or proliferating and dying at the same rate from days 8 to 10. The most mature population, p3, was the least viable. These cells remained MHC II^{high}, suggesting that they are short-lived, terminally differentiated cells.

To confirm proliferation of the HA binding population (p1), we labeled these cells with a cell proliferation dye CFSE that is diluted when the cells divide. Cells were cultured in the presence of GM-CSF with or without LPS for 3 d (Fig. 4B). LPS prevented the proliferation of this p1 population, providing a suitable negative control. In the absence of LPS, the p1, high HA binding MHC II^{mid/low} cells underwent a few rounds of division. In particular, it was the MHC II^{low} cells that underwent the greatest rounds of division. This confirms the HA binding population as a proliferative population and provides another distinction between this population and the immature and mature low HA binding MHC II^{mid} and MHC II^{high} DCs.

MHC II^{mid/low} HA binding BMDCs have morphological and phenotypic similarities to alveolar macrophages

Given that the HA binding population was F4/80⁺ and CD115⁺, CCR7⁻ and MHC II^{mid/low}, this raised the possibility that these

cells might be macrophages. Indeed, GM-CSF has been used to generate BMDMs (16). Furthermore, GM-CSF is important for the phenotype and function of alveolar macrophages in vivo (41, 42). To determine whether this HA binding population resembled alveolar macrophages, we compared the morphology and phenotype of p1–p3 BMDCs with that of alveolar macrophages. The BAL, which contains 80–95% alveolar macrophages, was plated alongside the sorted BMDC populations. Fig. 5A shows the alveolar macrophages as round and adherent; the HA binding MHC II^{mid/low} p1 cells as larger but with a smooth, round surface; the immature DCs (MHC II^{mid}, low HA binding) p2 cells were adherent and spread with more protrusions; whereas the mature DCs (MHC II^{high}, low HA binding) p3 cells were smaller, less adherent but extended many dendrites from the cell body. Although the p2 eventually develop dendrites over time, the HA binding p1 population never

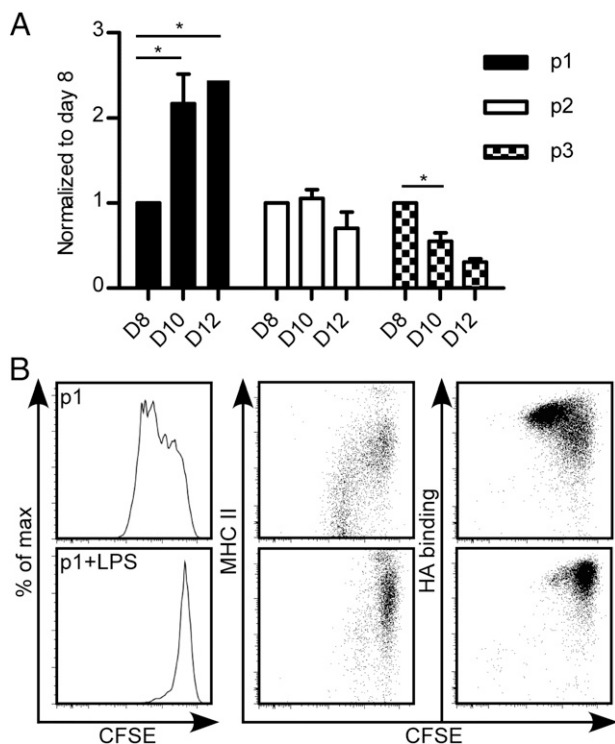


FIGURE 4. HA binding identifies a proliferative population. Day 7 C57BL/6J BMDCs were sorted for CD11c⁺ Gr1⁻, MHC II^{mid/low} high HA binding (p1), MHC II^{mid} low HA binding (p2), and MHC II^{high} low HA binding (p3) populations. Approximately 5×10^4 cells from each population were plated and further cultured with fresh GM-CSF. **(A)** Proliferation was measured by the fold change in cell number relative to the number of cells present on day 8. Graph shows an average of three mice from three experiments \pm SD with significance indicated as * $p < 0.05$, using paired t test. **(B)** HA binding BMDCs were labeled with the proliferation dye CFSE postsort and further cultured in the presence of GM-CSF with or without LPS for 5 d. MHC II expression and HA binding versus CFSE analyzed by flow cytometry. Plots are representative data, repeated three times, one mouse per experiment.

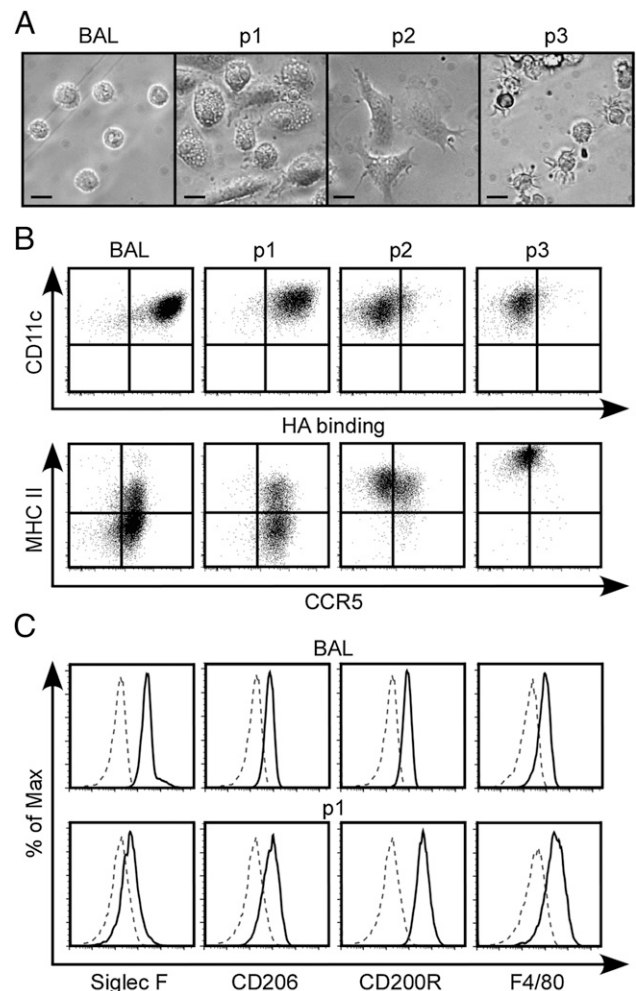


FIGURE 5. Morphology and phenotype of alveolar macrophages and BMDCs. **(A)** Day 7 C57BL/6J BMDCs were sorted for CD11c⁺ Gr1⁻ MHC II^{mid/low} HA binding^{high} (p1), MHC II^{mid} HA binding^{low} (p2), and MHC II^{high} HA binding^{low} (p3) populations. Cells from the BAL were collected from C57BL/6J mice. Approximately 5×10^4 cells were plated in a 96-well tissue culture plate for 2 h; then cell images were taken. This is a representative image, observed in least 50 cells in each experiment. Scale bar, 10 μ m. **(B)** Flow cytometry comparing CD11c expression and HA binding (top), and MHC II and CCR5 expression (bottom) between alveolar macrophages in the BAL and the different populations of BMDCs. **(C)** Histograms showing the expression of Siglec-F, CD206, CD200R, and F4/80 between alveolar macrophages in the BAL (top) and the HA binding, p1 BMDC population (bottom). Dotted line is the fluorescence minus one negative control. Data are from one representative experiment, repeated at least three times.

developed any dendrites from days 7 to 12 (data not shown). Although the morphology of each population was distinct, the p1 population most closely resembled that of the alveolar macrophages.

Strikingly, phenotypic analysis revealed that the alveolar macrophages bound FI-HA to a similar extent as p1 cells, expressed similar levels of CD11c and MHC II, and were CCR5⁺ (Fig. 5B). This distinguishes the p1 cells from the p2 and p3 populations, which have lower expression of CCR5 and higher levels of MHC II expression. Further comparison of the p1 population with the ex vivo alveolar macrophages revealed that the p1 population shared several markers with the alveolar macrophages. Alveolar macrophages are characterized by high Siglec-F, CD206, CD200R, and low F4/80 expression and the p1 cells mirrored this phenotype, except they had lower Siglec-F expression (Fig. 5C). Thus the high HA binding MHC II^{mid/low} p1 population within the BMDC culture shares morphological and phenotypic characteristics with alveolar macrophages.

LPS-activated MHC II^{mid/low} HA binding BMDCs and alveolar macrophages have different proinflammatory cytokine secretion profiles compared with mature DCs

To further determine whether the functional characteristics of this p1, MHC II^{mid/low} HA binding population were similar to that of alveolar macrophages and distinct from the mature DC population (p3), we compared their cytokine production after LPS stimulation. After 8 h of LPS stimulation, the p3 and p1 cell populations were gated as in Fig. 6A and analyzed for cytokine production (Fig. 6B). The majority of p1 cells made TNF- α and a proportion were making IL-6 or IL-12. It was noted that this cytokine production was not sustained as neither TNF- α nor IL-12 (IL-6 was not measured) was detected between 16 and 24 h after LPS stimulation (data not shown). In contrast, after 8-h LPS stimulation of the mature DC (p3) population, few cells were producing TNF- α or IL-6, but virtually all were producing IL-12 (Fig. 6B, 6C). Notably, ~50% of these cells were still making IL-12 between 16 and 24 h (data not shown). This provides further evidence that the HA binding p1 cells behave differently from mature BMDCs and supports the possibility that p1 cells are more macrophage-like, because they rapidly produce proinflammatory cytokines in response to LPS, whereas the mature DCs do not make TNF- α or IL-6 and instead have a sustained production of the T cell-polarizing cytokine, IL-12. When ex vivo alveolar macrophages were stimulated with LPS they also readily made TNF- α after 4-h stimulation but made very little IL-6 or IL-12 (Fig. 6D, 6E). Thus, the pattern of robust early TNF- α production in alveolar macrophages is most similar to the p1 BMDC population and distinct from the p3 population, suggesting that the p1 BMDCs are more similar to alveolar macrophages than mature BMDCs. These functional data, together with the phenotypic and morphological data, all support the conclusion that this HA binding BMDC population is distinct from the mature BMDC population and is most similar to ex vivo alveolar macrophages.

MHC II^{mid/low} HA binding cells, like alveolar macrophages, do not activate naive T cells

One of the major defining characteristics of a DC and what helps to distinguish it from a macrophage is its unique ability to activate naive T cells (2, 43). We therefore examined the ability of the high HA binding p1 population to activate naive T cells and compared their ability with the mature DCs (p3) and ex vivo alveolar macrophages. In this study, p1, p2, and p3 cells were sorted from day 7 CD11c⁺ Gr1⁻ BMDCs, stimulated with LPS, and loaded with OVA peptide for 24 h. LPS and OVA peptide were washed

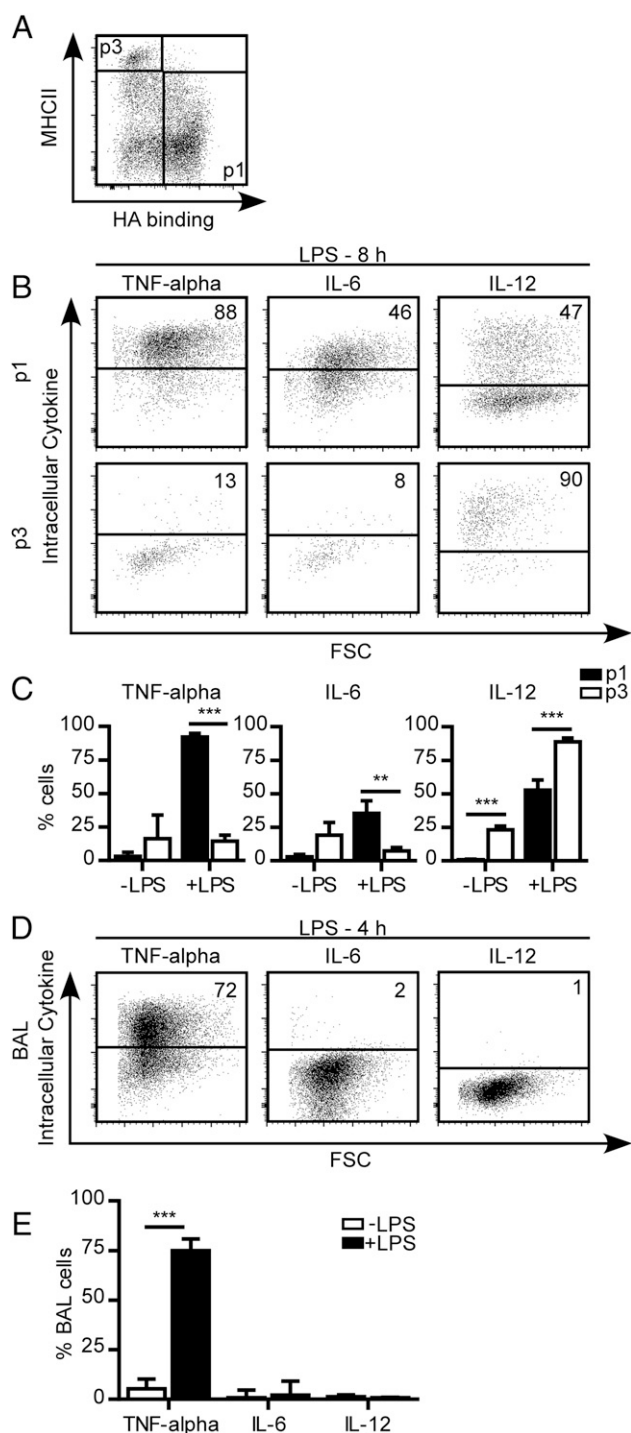


FIGURE 6. LPS-induced cytokine production from the BMDC populations and alveolar macrophages. Day 7 BMDC cultures were stimulated or not with LPS; then the populations were gated and analyzed for intracellular cytokine production by flow cytometry. (A) The gates used for the MHC II^{mid/low} HA binding^{high} (p1) and MHC II^{high} HA binding^{low} (p3) populations. (B) Intracellular TNF- α , IL-6, and IL-12 production after 8-h LPS stimulation with 6 h of brefeldin A in the p1 and p3 populations. (C) The percentage of TNF- α ⁺, IL-6⁺, and IL-12⁺ cells in p1 and p3 populations in the presence or absence of LPS. Graph is an average of six biological replicates over two experiments \pm SD with significance indicated as ** p < 0.01, *** p < 0.001, paired t test. (D) Intracellular cytokine production of ex vivo CD11c⁺ alveolar macrophages (BAL) after LPS stimulation. Intracellular TNF- α , IL-6, and IL-12 induced after 4 h of LPS stimulation and brefeldin A. (E) Proportion of TNF- α ⁺, IL-6⁺, and IL-12⁺ alveolar macrophages cultured with or without LPS. Graph is an average of three BAL samples from three experiments \pm SD, where each BAL sample was pooled from two mice. Significance is indicated as *** p < 0.001.

away before the cells were cocultured with CFSE-labeled naive CD4⁺ OT-II T cells. Three days later, T cell activation and proliferation were assessed by the upregulation of CD25 and CFSE dilution, respectively. LPS-stimulated p2 and p3 populations induced the majority of T cells to undergo several rounds of division, whereas the majority of T cells with the p1 population and the alveolar macrophages remained largely undivided (Fig. 7A). This translated into significant numbers of T cells being generated with the p2 and p3 populations, but not with the p1 or alveolar macrophage populations (Fig. 7B). Even without LPS stimulation, the p3 population was able to drive some proliferation, which is perhaps not too surprising, given their high level of MHC II and CD86 expression (Fig. 2A). Some T cell proliferation was also seen with the LPS-stimulated p2 population. This is consistent with the p2 population being the immature DC population, and their ability to mature rapidly into the mature DC (p3) population with LPS (Fig. 3D). These functional data provide strong evidence that the p1 BMDC population is not an immature or mature DC population; instead, it has all the hallmarks of a macrophage population and shows the most similarity to alveolar macrophages, which are dependent on GM-CSF for their development and maturation (11, 44, 45).

HA binding MHC II^{mid/low} cells are retained in the alveolar space, whereas low HA binding MHC II^{high} cells migrate to the lymph node upon LPS stimulation

HA is present in the lung around blood vessels and alveolar spaces (46). Because the HA binding cells in GM-CSF BMDC cultures were phenotypically and functionally more similar to alveolar macrophages (Figs. 5–7) than mature DCs, we wanted to deter-

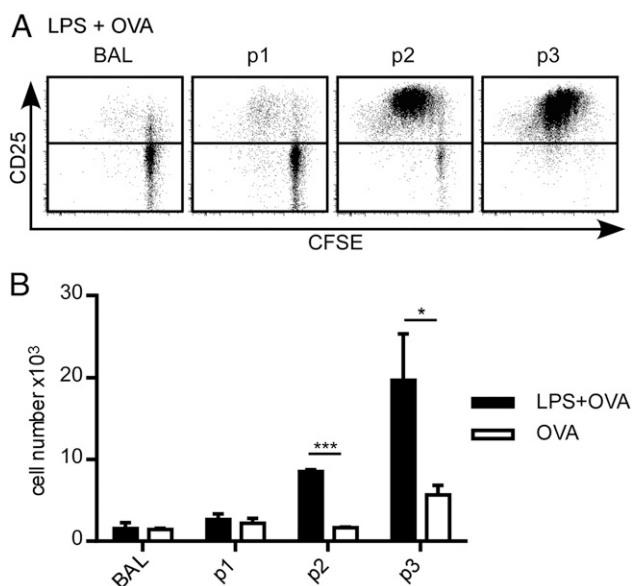


FIGURE 7. MHC II^{mid/low} HA binding BMDCs and alveolar macrophages do not activate T cells. **(A)** Cells collected from the BAL (alveolar macrophages) and day 7 BMDCs sorted for CD11c⁺ Gr1⁻, MHC II^{mid/low} HA binding^{high} (p1), MHC II^{mid} HA binding^{low} (p2), and MHC II^{high} HA binding^{low} (p3) populations were cultured with OVA peptide in the presence and absence of LPS overnight. After 24 h, the LPS and OVA peptide were washed away, and the APCs were cocultured with CFSE-labeled OT-II T cells for 3 d. OT-II T cell proliferation was analyzed by flow cytometry, where T cells were first gated by CD3 and then examined for CD25 and CFSE expression. **(B)** Number of T cells present after 3 d of DC and T cell coculture. Graph shows the average of triplicates \pm SD from one experiment. These are representative data repeated twice with one mouse each. * $p < 0.05$, *** $p < 0.001$.

mine whether they would behave like alveolar macrophages or DCs in vivo. GFP⁺ bone marrow cells (isolated from GFP⁺ mice) were cultured in the presence of GM-CSF for 8 d; then 5 million of the nonadherent cells in the culture were instilled into the lungs of C57BL/6J mice. Approximately 70% of this GFP⁺ BMDC population was CD11c⁺ cells that contained both immature and mature BMDCs, as well as the HA binding MHC II^{mid/low} population (Fig. 8A). After 24 h, 18% of the cells collected from the BAL were GFP⁺, of which 88% were CD11c⁺ Gr1⁻, and within the CD11c⁺ cells, 45% were now HA binding (Fig. 8B). This percentage increase from 11 to 45% of the HA binding population indicated that these cells were being selected for in this environment.

In the presence of inflammatory stimuli, DCs mature, upregulate CCR7 expression, and migrate to draining lymph nodes to activate the adaptive immune response, whereas macrophages are retained in tissues to control local infection (47). GFP⁺ BMDCs were instilled into the lung for 24 h, then LPS was instilled, and after another 24 h the cells were isolated from the BAL and the mediastinal lymph node and analyzed by flow cytometry. Consistent with the in vitro p1 phenotype, the majority of the CD11c⁺ Gr1⁻ GFP⁺ donor cells that remained in the alveolar space after LPS instillation were MHC II^{mid/low} and positive for HA binding (Fig. 8C, 8D), whereas the CD11c⁺ GFP⁺ cells that had migrated to the draining lymph node were MHC II^{high} low HA binding cells, similar to the phenotype observed in vitro for the mature DCs (Fig. 8C, 8E). These phenotypes were also similar to the GFP⁻ host cells residing in these two locations (Fig. 8C). Thus, the high HA binding, MHC II^{mid/low} BMDCs were acting like alveolar macrophages and the cells migrating to the local lymph node had features consistent with mature DCs. We conclude that the HA binding MHC II^{mid/low} population in BMDC cultures closely resembles alveolar macrophages. This provides a simple and unique way to distinguish GM-CSF-induced macrophages from GM-CSF-induced DCs and provides a suitable in vitro system to generate and model alveolar macrophages.

Discussion

In this study, we have identified a subpopulation of CD11c⁺ MHC II^{mid/low} macrophage-like cells that bind high levels of HA in murine GM-CSF BMDC cultures. In the absence of HA binding, they are difficult to distinguish from immature BMDCs, yet they are distinct from immature and mature DCs by functional criteria. They have a distinct morphology and readily produce TNF- α and some IL-6 and IL-12 in response to LPS but are unable to activate naive T cells. This contrasts with the mature DCs that did not make TNF- α and instead showed sustained production of IL-12 in response to LPS and activated naive T cells. This is consistent with macrophages being able to respond rapidly to pathogens in the tissues, whereas the sustained production of IL-12 is more relevant for mature DCs that have migrated to the draining lymph node. Previously, it had not been appreciated that subpopulations of BMDC cultures make specific cytokines in response to TLR stimulation. In this study, we have been able to dissect the BMDCs into at least two distinct populations: the HA binding macrophage-like cells that rapidly make inflammatory cytokines and the mature DCs that produce sustained levels of the Th1 polarizing cytokine, IL-12. When BMDCs were instilled into the alveolar space and subsequently challenged with LPS, the HA binding population was retained in the alveolar space, whereas the low HA binding MHC II^{high} DCs migrated to the mediastinal lymph node. This further supports our conclusion that the HA binding cells are macrophages that stay in the tissue and fight infection by producing local

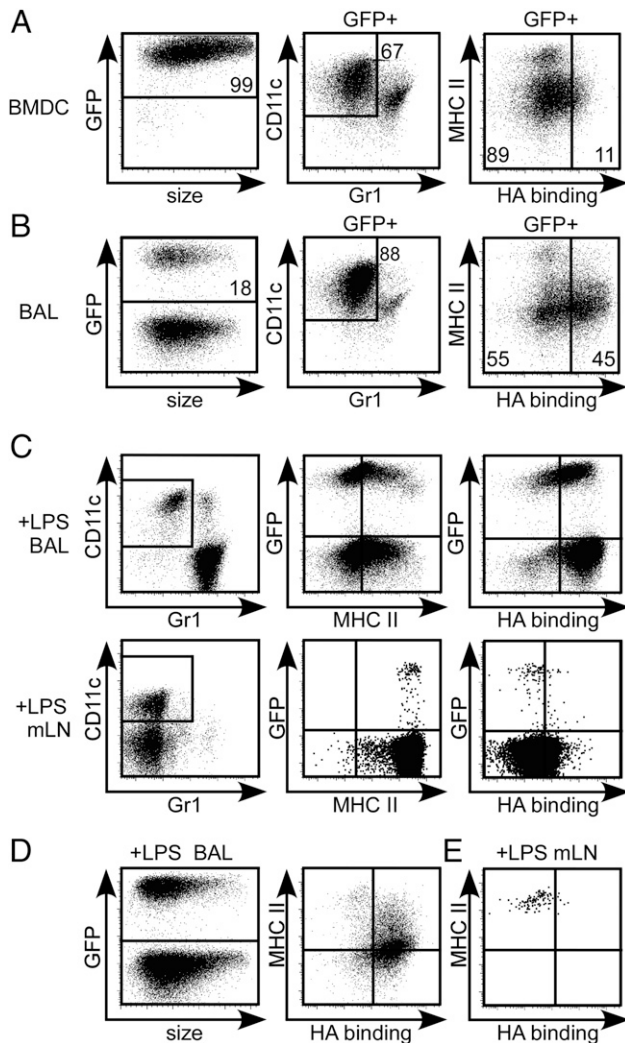


FIGURE 8. MHC II^{mid/low} HA binding cells are retained in the alveolar space, whereas the MHC II^{high} low HA binding cells migrate to the lymph node after LPS-induced lung inflammation. **(A)** GFP⁺ CD11c⁺ Gr1⁻ cells were gated, and the proportion of HA binding cells before instillation was analyzed. **(B)** A total of 5×10^6 day 8 GFP⁺ BMDCs was instilled into the lung and the BAL was analyzed after 24 h. **(C)** Twenty-four hours after the cells were instilled into the lung, LPS (25 μ g/50 μ l) was injected via intratracheal instillation. Twenty-four hours after LPS stimulation, the BAL (*top*) and mediastinal lymph node (mLN, *bottom*) were analyzed. **(D)** and **(E)** After LPS treatment, CD11c⁺ Gr1⁻ cells were gated, and GFP⁺ donor cells identified and analyzed for MHC II expression and HA binding in the BAL (**D**) and mLN (**E**). This is one representative experiment that was repeated at least three times.

proinflammatory cytokines, whereas the DCs migrate to the lymph node where they present Ag to T cells and secrete T cell–polarizing cytokines.

LPS did upregulate MHC II expression from mid/low to mid and did upregulate CD40 expression and, to a lesser extent, CD86 costimulatory molecule expression (data not shown) in the p1 macrophage-like population, but this was still insufficient to activate naive T cells. This intermediate level of MHC II expression may be sufficient to present Ag and activate memory T cells, but this was not tested.

It was somewhat surprising to find a macrophage population in the nonadherent fraction of the BMDC culture. GM-CSF bone marrow cultures have been used to generate BMDCs and BMDMs, and the main difference between the two methods has been to

collect the nonadherent fraction for DCs and the adherent fraction for macrophages (16, 18). Examination of the adherent fraction of the day 7/8 culture showed similar CD11c⁺ cell populations: p0: MHC II^{low}, p1: MHC II^{mid/low} HA binding^{high}, and p2: MHC II^{mid} HA binding^{low}, but a notable absence of the p3: MHC II^{high} mature DC population (data not shown). The percentage of the p1 population was slightly enriched in the adherent fraction compared with the nonadherent fraction. Following the GM-CSF BMDM protocol, the adherent cells were made up of the same populations, p0, p1, and p2 with essentially no p3, showing no obvious difference between the adherent cells in the BMDC culture (data not shown). This implies that neither the *in vitro* BMDM nor BMDC cultures are a pure population, and that both are a mix of macrophages and immature DCs. During this study it was noted that the percentage of the HA binding population varied slightly with different batches of serum, suggesting that factors in the serum may influence the type of cell that is produced.

In a comparison between Flt3-derived BMDCs and GM-CSF/IL-4-derived BMDCs, it was concluded that the Flt3-derived DCs best resemble conventional lymph node resident DCs, whereas GM-CSF/IL-4-derived DCs are the equivalent of TNF- α and inducible NO synthase–producing DCs that emerge after inflammation *in vivo* (24). Our work shows that GM-CSF–induced BMDCs are a heterogeneous population consisting of at least the immature and mature DCs that resemble the conventional DCs, as well as a distinct macrophage population capable of producing TNF- α upon TLR-4 stimulation. In this study, we have not explored the origin of these DC and macrophage populations, whether they both arise from a common macrophage-DC progenitor or whether they arise separately from a distinct DC progenitor and a distinct monocyte progenitor. However, recent data indicate that conventional DCs and macrophages arise from distinct progenitors in the bone marrow and do not share a common macrophage-DC progenitor (48), as was originally thought (49). Whether FI-HA can also be used to distinguish macrophage progenitors in the bone marrow remains to be addressed. Although the percentage of HA binding cells in the bone marrow is low, 3–4 d after culture in GM-CSF, the majority (85%) of HA binding cells are found within the CD115⁺ population, consistent with marking a macrophage progenitor. Although the HA binding population increases within the CD115⁺ population during development, not all CD115⁺ cells in the bone marrow culture bind HA (data not shown), making it unclear whether FI-HA marks a subset of these cells or is just induced at a specific stage of their differentiation. Because the bone marrow CD11c⁺, low FI-HA binding, low MHC II, p0 population can give rise to both high and low HA populations, it suggests that the high HA binding macrophages come from a low FI-HA binding progenitor cell. However, once the CD11c⁺ cells upregulate FI-HA binding, although they can still proliferate in response to GM-CSF, they are macrophage-like and unable to give rise to mature DCs.

This GM-CSF–derived p1 macrophage population most closely resembles alveolar macrophages, which are known to be CD11c⁺, bind HA, can self-renew (11, 41, 50), and depend on GM-CSF for their differentiation (45). Despite the p1 cells arising from GM-CSF cultured bone marrow cells, they are, like the alveolar macrophages, positive for CD200R and CD206, two markers associated with alternatively activated macrophages. This is consistent with alveolar macrophages having a scavenger role to remove debris and repair damage. However, they can also respond rapidly to LPS by producing TNF- α , indicating that alveolar macrophages share elements of both M1 and M2 polarized macrophages. These functions are consistent with a sentinel role for alveolar macrophages, which can remove debris and repair damage

without evoking an inflammatory response, yet are capable of doing so should they encounter microbes.

Although there are several phenotypic and functional similarities between the p1 population and alveolar macrophages, there are subtle differences in the phenotype of p1 BMDCs that suggest they may best represent an immature alveolar macrophage, as the p1 cells are CD11b⁺, CD11c^{high}, Siglec-F^{low} and mature alveolar macrophages are CD11b^{lo}, CD11c^{high}, and Siglec-F^{high}. Notably, alveolar macrophages soon gain CD11b when they are grown in culture (Y. Dong, unpublished observations). Despite this, this p1 subset of BMDCs still represents one of the best in vitro-derived alveolar macrophage-like cells to date that can be obtained readily in relatively large numbers. Because the numbers of murine alveolar macrophages one can obtain for in vitro studies are limited, and previous in vitro culture methods to generate alveolar-like macrophages are time consuming (51), HA binding combined with MHC II^{mid/low} expression provides an easy way to isolate macrophages from BMDC cultures that can be used to model alveolar macrophages.

Why BMDM and alveolar macrophages bind HA to a much greater extent than DCs is not understood. HA is a major component of the extracellular matrix present in most tissues including the lung where it is found around the blood vessels and alveolar spaces (46). HA may provide a means of retaining macrophages in the tissue. Indeed, we observed that the high HA binding CCR5⁺ cells were less migratory to CCL3 than the low HA binding CCR5⁺ cells. HA-rich niches have also been proposed in the bone marrow, although there it is thought to provide a supportive niche environment for hematopoietic stem cells (52, 53). Further work is needed to understand the significance of HA binding by these GM-CSF-induced macrophages. In this study, the ability of GM-CSF-induced macrophages to bind HA distinguishes them from immature DCs and coupled with MHC II^{mid/low} expression provides a simple way of identifying macrophages in GM-CSF BMDC cultures that were previously thought to generate only DCs. It also provides a useful means to isolate these cells, which can be used in vitro to model alveolar macrophages.

Acknowledgments

We acknowledge support from UBC Flow Cytometry Facility and thank Dr. Fabio Rossi for the GFP⁺ mice.

Disclosures

The authors have no financial conflicts of interest.

References

- Murray, P. J., and T. A. Wynn. 2011. Protective and pathogenic functions of macrophage subsets. *Nat. Rev. Immunol.* 11: 723–737.
- Merad, M., P. Sathe, J. Helft, J. Miller, and A. Mortha. 2013. The dendritic cell lineage: ontogeny and function of dendritic cells and their subsets in the steady state and the inflamed setting. *Annu. Rev. Immunol.* 31: 563–604.
- Mosser, D. M., and J. P. Edwards. 2008. Exploring the full spectrum of macrophage activation. *Nat. Rev. Immunol.* 8: 958–969.
- Soehnlein, O., and L. Lindbom. 2010. Phagocyte partnership during the onset and resolution of inflammation. *Nat. Rev. Immunol.* 10: 427–439.
- Steinman, R. M., and J. Banchereau. 2007. Taking dendritic cells into medicine. *Nature* 449: 419–426.
- Hashimoto, D., J. Miller, and M. Merad. 2011. Dendritic cell and macrophage heterogeneity in vivo. *Immunity* 35: 323–335.
- Geissmann, F., S. Gordon, D. A. Hume, A. M. Mowat, and G. J. Randolph. 2010. Unravelling mononuclear phagocyte heterogeneity. *Nat. Rev. Immunol.* 10: 453–460.
- Hume, D. A., N. Mabbott, S. Raza, and T. C. Freeman. 2013. Can DCs be distinguished from macrophages by molecular signatures? *Nat. Immunol.* 14: 187–189.
- Randolph, G., and M. Merad. 2013. Reply to: "Can DCs be distinguished from macrophages by molecular signatures?". *Nat. Immunol.* 14: 189–190.
- Ruffell, B., G. F. Poon, S. S. Lee, K. L. Brown, S. L. Tjewa, J. Cooper, and P. Johnson. 2011. Differential use of chondroitin sulfate to regulate hyaluronan binding by receptor CD44 in Inflammatory and Interleukin 4-activated Macrophages. *J. Biol. Chem.* 286: 19179–19190.
- Hussell, T., and T. J. Bell. 2014. Alveolar macrophages: plasticity in a tissue-specific context. *Nat. Rev. Immunol.* 14: 81–93.
- Miller, J. C., B. D. Brown, T. Shay, E. L. Gautier, V. Jojic, A. Cohain, G. Pandey, M. Leboeuf, K. G. Elpek, J. Helft, et al. Immunological Genome Consortium. 2012. Deciphering the transcriptional network of the dendritic cell lineage. *Nat. Immunol.* 13: 888–899.
- Vermaelen, K., and R. Pauwels. 2004. Accurate and simple discrimination of mouse pulmonary dendritic cell and macrophage populations by flow cytometry: methodology and new insights. *Cytometry A* 61: 170–177.
- Gautier, E. L., T. Shay, J. Miller, M. Greter, C. Jakubzick, S. Ivanov, J. Helft, A. Chow, K. G. Elpek, S. Gordonov, et al. Immunological Genome Consortium. 2012. Gene-expression profiles and transcriptional regulatory pathways that underlie the identity and diversity of mouse tissue macrophages. *Nat. Immunol.* 13: 1118–1128.
- Tamoutounour, S., S. Henri, H. Lelouard, B. de Bovis, C. de Haar, C. J. van der Woude, A. M. Woltman, Y. Reyat, D. Bonnet, D. Sichien, et al. 2012. CD64 distinguishes macrophages from dendritic cells in the gut and reveals the Th1-inducing role of mesenteric lymph node macrophages during colitis. *Eur. J. Immunol.* 42: 3150–3166.
- Fleetwood, A. J., T. Lawrence, J. A. Hamilton, and A. D. Cook. 2007. Granulocyte-macrophage colony-stimulating factor (CSF) and macrophage CSF-dependent macrophage phenotypes display differences in cytokine profiles and transcription factor activities: implications for CSF blockade in inflammation. *J. Immunol.* 178: 5245–5252.
- Inaba, K., M. Inaba, N. Romani, H. Aya, M. Deguchi, S. Ikehara, S. Muramatsu, and R. M. Steinman. 1992. Generation of large numbers of dendritic cells from mouse bone marrow cultures supplemented with granulocyte/macrophage colony-stimulating factor. *J. Exp. Med.* 176: 1693–1702.
- Lutz, M. B., N. Kukutsch, A. L. Ogilvie, S. Rössner, F. Koch, N. Romani, and G. Schuler. 1999. An advanced culture method for generating large quantities of highly pure dendritic cells from mouse bone marrow. *J. Immunol. Methods* 223: 77–92.
- Brasel, K., H. J. McKenna, K. Charrier, P. J. Morrissey, D. E. Williams, and S. D. Lyman. 1997. Flt3 ligand synergizes with granulocyte-macrophage colony-stimulating factor or granulocyte colony-stimulating factor to mobilize hematopoietic progenitor cells into the peripheral blood of mice. *Blood* 90: 3781–3788.
- Lacey, D. C., A. Achuthan, A. J. Fleetwood, H. Dinh, J. Roiniotis, G. M. Scholz, M. W. Chang, S. K. Beckman, A. D. Cook, and J. A. Hamilton. 2012. Defining GM-CSF- and macrophage-CSF-dependent macrophage responses by in vitro models. *J. Immunol.* 188: 5752–5765.
- Sallusto, F., and A. Lanzavecchia. 1994. Efficient presentation of soluble antigen by cultured human dendritic cells is maintained by granulocyte/macrophage colony-stimulating factor plus interleukin 4 and downregulated by tumor necrosis factor alpha. *J. Exp. Med.* 179: 1109–1118.
- Naik, S. H., P. Sathe, H.-Y. Park, D. Metcalf, A. I. Proietto, A. Dakic, S. Carotta, M. O'Keeffe, M. Bahlo, A. Papenfuss, et al. 2007. Development of plasmacytoid and conventional dendritic cell subtypes from single precursor cells derived in vitro and in vivo. *Nat. Immunol.* 8: 1217–1226.
- Shortman, K., and S. H. Naik. 2007. Steady-state and inflammatory dendritic-cell development. *Nat. Rev. Immunol.* 7: 19–30.
- Xu, Y., Y. Zhan, A. M. Lew, S. H. Naik, and M. H. Kershaw. 2007. Differential development of murine dendritic cells by GM-CSF versus Flt3 ligand has implications for inflammation and trafficking. *J. Immunol.* 179: 7577–7584.
- Levesque, M. C., and B. F. Haynes. 1997. Cytokine induction of the ability of human monocyte CD44 to bind hyaluronan is mediated primarily by TNF-alpha and is inhibited by IL-4 and IL-13. *J. Immunol.* 159: 6184–6194.
- Fraser, J. R., T. C. Laurent, and U. B. Laurent. 1997. Hyaluronan: its nature, distribution, functions and turnover. *J. Intern. Med.* 242: 27–33.
- Jiang, D., J. Liang, and P. W. Noble. 2007. Hyaluronan in tissue injury and repair. *Annu. Rev. Cell Dev. Biol.* 23: 435–461.
- Teder, P., R. W. Vandivier, D. Jiang, J. Liang, L. Cohn, E. Puré, P. M. Henson, and P. W. Noble. 2002. Resolution of lung inflammation by CD44. *Science* 296: 155–158.
- Ruffell, B., and P. Johnson. 2009. The regulation and function of hyaluronan binding by CD44 in the immune system. *Glycoforum. Science of hyaluronan today*. Available at: <http://www.glycoforum.gr.jp/science/hyaluronan/HA32/HA32E.html>.
- Johnson, P., and B. Ruffell. 2009. CD44 and its role in inflammation and inflammatory diseases. *Inflamm. Allergy Drug Targets* 8: 208–220.
- Levesque, M. C., and B. F. Haynes. 1999. TNF-alpha and IL-4 regulation of hyaluronan binding to monocyte CD44 involves posttranslational modification of CD44. *Cell. Immunol.* 193: 209–218.
- Termeer, C. C., J. Hennies, U. Voith, T. Ahrens, J. M. Weiss, P. Prehm, and J. C. Simon. 2000. Oligosaccharides of hyaluronan are potent activators of dendritic cells. *J. Immunol.* 165: 1863–1870.
- Termeer, C., F. Benedix, J. Sleeman, C. Fieber, U. Voith, T. Ahrens, K. Miyake, M. Freudenberg, C. Galanos, and J. C. Simon. 2002. Oligosaccharides of Hyaluronan activate dendritic cells via toll-like receptor 4. *J. Exp. Med.* 195: 99–111.
- Mummert, M. E., D. Mummert, D. Edelbaum, F. Hui, H. Matsue, and A. Takashima. 2002. Synthesis and surface expression of hyaluronan by dendritic cells and its potential role in antigen presentation. *J. Immunol.* 169: 4322–4331.
- Schmits, R., J. Filmus, N. Gerwin, G. Senaldi, F. Kiefer, T. Kundig, A. Wakeham, A. Shahinian, C. Catzavelos, J. Rak, et al. 1997. CD44 regulates

- hematopoietic progenitor distribution, granuloma formation, and tumorigenicity. *Blood* 90: 2217–2233.
36. Stockinger, B., T. Zal, A. Zal, and D. Gray. 1996. B cells solicit their own help from T cells. *J. Exp. Med.* 183: 891–899.
 37. de Belder, A. N., and K. O. Wik. 1975. Preparation and properties of fluorescein-labelled hyaluronate. *Carbohydr. Res.* 44: 251–257.
 38. Liang, J., D. Jiang, J. Griffith, S. Yu, J. Fan, X. Zhao, R. Bucala, and P. W. Noble. 2007. CD44 is a negative regulator of acute pulmonary inflammation and lipopolysaccharide-TLR signaling in mouse macrophages. *J. Immunol.* 178: 2469–2475.
 39. Bachmann, M. F., M. Kopf, and B. J. Marsland. 2006. Chemokines: more than just road signs. *Nat. Rev. Immunol.* 6: 159–164.
 40. Kato, M., T. K. Neil, D. B. Fearnley, A. D. McLellan, S. Vuckovic, and D. N. Hart. 2000. Expression of multilectin receptors and comparative FITC-dextran uptake by human dendritic cells. *Int. Immunol.* 12: 1511–1519.
 41. Guth, A. M., W. J. Janssen, C. M. Bosio, E. C. Crouch, P. M. Henson, and S. W. Dow. 2009. Lung environment determines unique phenotype of alveolar macrophages. *Am. J. Physiol. Lung Cell. Mol. Physiol.* 296: L936–L946.
 42. Paine, R., III, S. B. Morris, H. Jin, S. E. Wilcoxon, S. M. Phare, B. B. Moore, M. J. Coffey, and G. B. Toews. 2001. Impaired functional activity of alveolar macrophages from GM-CSF-deficient mice. *Am. J. Physiol. Lung Cell. Mol. Physiol.* 281: L1210–L1218.
 43. Steinman, R. M., and M. D. Witmer. 1978. Lymphoid dendritic cells are potent stimulators of the primary mixed leukocyte reaction in mice. *Proc. Natl. Acad. Sci. USA* 75: 5132–5136.
 44. Stanley, E., G. J. Lieschke, D. Grail, D. Metcalf, G. Hodgson, J. A. Gall, D. W. Maher, J. Cebon, V. Sinickas, and A. R. Dunn. 1994. Granulocyte/macrophage colony-stimulating factor-deficient mice show no major perturbation of hematopoiesis but develop a characteristic pulmonary pathology. *Proc. Natl. Acad. Sci. USA* 91: 5592–5596.
 45. Guilleams, M., I. De Kleer, S. Henri, S. Post, L. Vanhoutte, S. De Prijck, K. Deswarte, B. Malissen, H. Hammad, and B. N. Lambrecht. 2013. Alveolar macrophages develop from fetal monocytes that differentiate into long-lived cells in the first week of life via GM-CSF. *J. Exp. Med.* 210: 1977–1992.
 46. Cheng, G., S. Swaidani, M. Sharma, M. E. Lauer, V. C. Hascall, and M. A. Aronica. 2011. Hyaluronan deposition and correlation with inflammation in a murine ovalbumin model of asthma. *Matrix Biol.* 30: 126–134.
 47. Jakubzick, C., F. Tacke, J. Llodra, N. van Rooijen, and G. J. Randolph. 2006. Modulation of dendritic cell trafficking to and from the airways. *J. Immunol.* 176: 3578–3584.
 48. Sathe, P., D. Metcalf, D. Vremec, S. H. Naik, W. Y. Langdon, N. D. Huntington, L. Wu, and K. Shortman. 2014. Lymphoid tissue and plasmacytoid dendritic cells and macrophages do not share a common macrophage-dendritic cell-restricted progenitor. *Immunity* 41: 104–115.
 49. Auffray, C., D. K. Fogg, E. Narni-Mancinelli, B. Senechal, C. Trouillet, N. Saederup, J. Leemput, K. Bigot, L. Campisi, M. Abitbol, et al. 2009. CX3CR1+ CD115+ CD135+ common macrophage/DC precursors and the role of CX3CR1 in their response to inflammation. *J. Exp. Med.* 206: 595–606.
 50. Culty, M., H. A. Nguyen, and C. B. Underhill. 1992. The hyaluronan receptor (CD44) participates in the uptake and degradation of hyaluronan. *J. Cell Biol.* 116: 1055–1062.
 51. Fejer, G., M. D. Wegner, I. Györy, I. Cohen, P. Engelhard, E. Voronov, T. Manke, Z. Ruzsics, L. Dölken, O. Prazeres da Costa, et al. 2013. Nontransformed, GM-CSF-dependent macrophage lines are a unique model to study tissue macrophage functions. *Proc. Natl. Acad. Sci. USA* 110: E2191–E2198.
 52. Goncharova, V., N. Seroby, S. Iizuka, I. Schraufstatter, A. de Ridder, T. Povaliy, V. Wacker, N. Itano, K. Kimata, I. A. Orlovskaja, et al. 2012. Hyaluronan expressed by the hematopoietic microenvironment is required for bone marrow hematopoiesis. *J. Biol. Chem.* 287: 25419–25433.
 53. Nilsson, S. K., D. N. Haylock, H. M. Johnston, T. Occhiodoro, T. J. Brown, and P. J. Simmons. 2003. Hyaluronan is synthesized by primitive hemopoietic cells, participates in their lodgment at the endosteum following transplantation, and is involved in the regulation of their proliferation and differentiation in vitro. *Blood* 101: 856–862.